Available online at www.sciencedirect.com
ScienceDirect
Phytochemistry 68 (2007) 2043–2052
PHYTOCHEMISTRY
www.elsevier.com/locate/phytochem

Salicylate and catechol levels are maintained in *nahG* transgenic poplar

Alison M. Morse [a,*], Timothy J. Tschaplinski [b], Christopher Dervinis [a], Paula M. Pijut [c], Eric A. Schmelz [d], Wendy Day [a], John M. Davis [a,e]

[a] *School of Forest Resources and Conservation, University of Florida, P.O. Box 110410, Gainesville, FL 32611, United States*
[b] *Environmental Sciences Division, Oak Ridge National Laboratory, Oak Ridge, TN 37831, United States*
[c] *Hardwood Tree Improvement & Regeneration Center, Northern Research Station, USDA Forest Service, West Lafayette, IN 47907, United States*
[d] *Chemistry Research Unit, USDA Agricultural Research Service, Gainesville, FL 32608, United States*
[e] *Genetics Institute, University of Florida, P.O. Box 110410, Gainesville, FL 32611, United States*

Received 22 September 2006; received in revised form 28 April 2007
Available online 27 June 2007

Abstract

Metabolic profiling was used to investigate the molecular phenotypes of a transgenic *Populus tremula* × *P. alba* hybrid expressing the *nahG* transgene, a bacterial gene encoding salicylate hydroxylase that converts salicylic acid to catechol. Despite the efficacy of this transgenic approach to reduce salicylic acid levels in other model systems and thereby elucidate roles for salicylic acid in plant signaling, transgenic poplars had similar foliar levels of salicylic acid and catechol to that of non-transformed controls and exhibited no morphological phenotypes. To gain a deeper understanding of the basis for these observations, we analyzed metabolic profiles of leaves as influenced by transgene expression. Expression of *nahG* decreased quinic acid conjugates and increased catechol glucoside, while exerting little effect on levels of salicylic acid and catechol, the substrate and product, respectively, of the *nahG* enzyme. This suggests a biological role of elevated constitutive salicylic acid levels in *Populus*, in contrast to other plant systems in which *nahG* dramatically reduces salicylic acid levels.

Keywords: *Populus tremula* × *P. alba* hybrid; Salicaceae; Phenolic glycoside; Catechol; Quinic acid; Salicylic acid; Salicylate hydroxylase; *nahG*

1. Introduction

Salicylates are carbon-based secondary metabolites prominent in willow (*Salix* sp.) and poplar (*Populus* sp.) trees, members of the Salicaceae family. Both poplars and willows have been exploited by pre-industrial cultures as sources of salicin, a salicylate derivative and aspirin precursor, for treatment of pain, fever and headaches. While salicylates are found in plants other than the Salicaceae, many salicin derivatives appear to be characteristic of members of the Salicaceae. Significant foliar amounts of salicylate phenolic glycosides, primarily salireposide, trichocarpin, salicin, salicortin and tremulacin, have been quantified in various *Populus* species (Pearl and Darling, 1971; Thieme and Benecke, 1971). Total concentrations of salicylates in members of the Salicaceae have been found to range from 1% to 20% on a dry mass basis (Julkunen-Tiitto, 1989).

Research interest in the role of salicylates in plants, particularly salicylic acid **1** (SA), is of particular interest because of its involvement in disease resistance, pathogenesis-related gene expression, and the hypersensitive response (Delaney et al., 1994; Kunkel and Brooks, 2002). An important study demonstrating the role of SA **1** in plant defense involved ectopic over-expression of bacterial salicylate hydroxylase encoded by the *Pseudomonas nahG* gene (Gaffney et al., 1993). In transgenic tobacco and *Arabidopsis* plants, ectopic *nahG* expression prevents accumulation of SA **1** by catalyzing the oxidative decarboxylation of SA **1** to catechol **2**, resulting in increased susceptibility to disease and suppression of systemic acquired

* Corresponding author. Tel.: +1 352 273 8123; fax: +1 352 273 8284.
E-mail address: ammorse@ufl.edu (A.M. Morse).

0031-9422/$ - see front matter © 2007 Elsevier Ltd. All rights reserved.
doi:10.1016/j.phytochem.2007.05.014

resistance (Friedrich et al., 1995; Gaffney et al., 1993; Uknes et al., 1993). Recent work, showing that *nahG* expression can alter host defense pathways independent of its role in the removal of SA **1**, demonstrates the need for further investigation into the relative importance of catechol **2** accumulation, either alone or in combination with SA **1** depletion, in altering plant defense responses (Heck et al., 2003; van Wees and Glazebrook, 2003). In addition to defense responses, other roles for SA **1**, or for elevated catechol **2** levels resulting from the activity of salicylate hydroxylase on SA **1**, have been elucidated using *nahG* transgenics. *nahG* transgenic *Arabidopsis* plants had reduced tolerance to drought (Chini et al., 2004) and delayed leaf chlorosis during senescence (Morris et al., 2000), while transgenic tobacco plants had increased ozone tolerance (Orvar et al., 1997).

Molecular techniques such as metabolic profiling can assist in the functional investigation of transgenics with 'silent' phenotypes (i.e. no visible manifestation of the genetic modification) since genetic modifications are expected to often affect biochemical pathways. While traditional approaches to quantifying small molecules have targeted single metabolites, metabolic profiling provides a snapshot of the levels of many small molecules within a tissue and how the levels change under various circumstances, including different genetic compositions. Metabolic profiling has been used in *Saccharomyces cerevisiae* to identify the site of action for genes which, when deleted, have no measurable effect on growth (Allen et al., 2003; Raamsdonk et al., 2001), as well as to define silent morphological phenotypes in potato plants (Weckwerth et al., 2004). In transgenic poplar, broad spectrum profiling established the metabolic phenotypes of *gai* and *rgl1* mutants (that lack a gibberellin DELLA domain) as having reduced carbon flux through the lignin biosynthetic pathway with a shift towards allocation of secondary compounds to storage and defense metabolites, including various phenolics (Busov et al., 2006). Thus, metabolic profiling can identify biochemical phenotypes and be used to infer pathways that are disrupted based on the class of metabolites that are altered.

Given the important role of SA **1** in defense signaling in herbaceous plants and the high constitutive levels of SA **1** in poplar trees, we investigated the possibility that altering SA **1** levels in poplars could establish a biological role for this metabolite in this clade of forest trees. Our overall goal was, therefore, to perturb endogenous SA **1** levels in poplar; however, the biosynthetic pathway leading to SA **1** can vary among species (Metraux, 2002) and has not been determined in poplar. Because transgenic manipulation of endogenous SA **1** biosynthetic genes in poplar was therefore not a realistic option, we introduced a bacterial transgene encoding salicylate hydroxlase (NahG), a strategy that has been successful in reducing endogenous SA **1** in other plant systems. However, we detected neither a reduction in SA **1** nor an increase in catechol **2** levels in *nahG* transgenic lines, nor did we find a morphological phenotype in these lines. To obtain clues as to why SA **1** and catechol **2** levels remained constant in transgenic *nahG* lines, we conducted metabolic profiling to explore levels of soluble metabolites that might be perturbed in the transgenics compared to non-transgenic controls. Such assays can suggest possible explanations for silent phenotypes (Cutler and McCourt, 2005). The results from the metabolic profiling of *nahG* transgenic poplars established alterations in the levels of metabolites in the shikimate and phenylpropanoid pathways, as well as compounds related to SA **1** and catechol **2**, including catechol glycoside **3**.

2. Results and discussion

2.1. Evaluation of nahG transgene expression in poplar

We regenerated 56 independent transgenic lines of a hybrid poplar clone, INRA 717 1-B4 (*Populus tremula* × *P. alba*) after *Agrobacterium*-mediated transformation with the *nahG* transgene. Presence of the transgene was assayed and confirmed for 24 of 26 randomly selected lines using primers against the *nahG* coding sequence. To evaluate *nahG* expression levels in various tissues (apex, young leaves, mature leaves, phloem and xylem), five biological replicates of each transgenic line and a non-transgenic control line (NT) were assayed for *nahG* transcript abundance. In all transgenic lines, *nahG* transcript abundance was higher in mature leaves than any other tissue (data not shown), thus mature leaves were used in all subsequent experiments. Northern blot hybridization of mature leaf samples from four transgenic lines (6A, 6H, 6E and 3H) were selected to represent a range of high and low transgene expression (Fig. 1a). No growth differences were apparent (Fig. 1b).

2.2. Endogenous SA levels are unchanged in the nahG transgenic lines

To determine whether *nahG* expression reduced the levels of endogenous salicylate, leaf tissues from three biological replicates from each of the selected transgenic lines and NT control were subjected to metabolite analysis using gas chromatography–mass spectrometry (GC–MS) with electron impact ionization. None of the assayed *nahG* transgenic lines displayed any substantial reductions in SA **1** levels nor were catechol **2** levels, the product of *nahG* catalytic activity, elevated (Fig. 2a). Thus, no correlation was detected between the levels of SA **1** or catechol **2** and *nahG* transcript abundance. The lack of reduction in SA levels could be the result of a failure to accumulate sufficient nahG protein to appreciably impact endogenous SA concentrations – the specific cells and compartments that accumulate SA **1** have not been characterized in detail. However, another possibility to consider is that consistent levels of SA **1** and catechol **2** in *nahG*-expressing poplars may arise from the tuning of enzyme activities in secondary

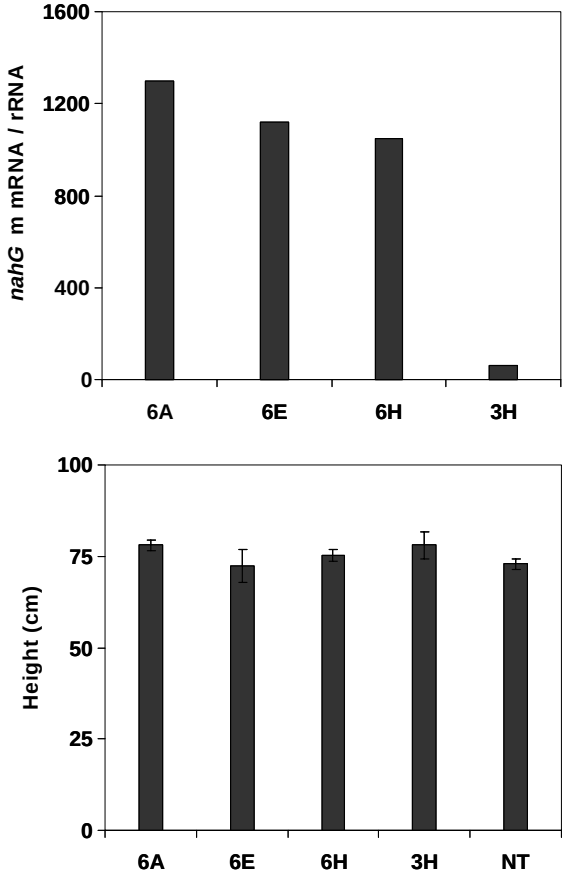

Fig. 1. Line-specific variations in *nahG* transcript abundance. (a) Data from a representative northern blot of *nahG* transgene expression relative to rRNA for four independent transgenic lines. (b) Height given is mean (cm) ± SE for three biological replicates per line. 6A, 6E, 6H and 3H are independent transgenic lines. NT is non-transgenic control line.

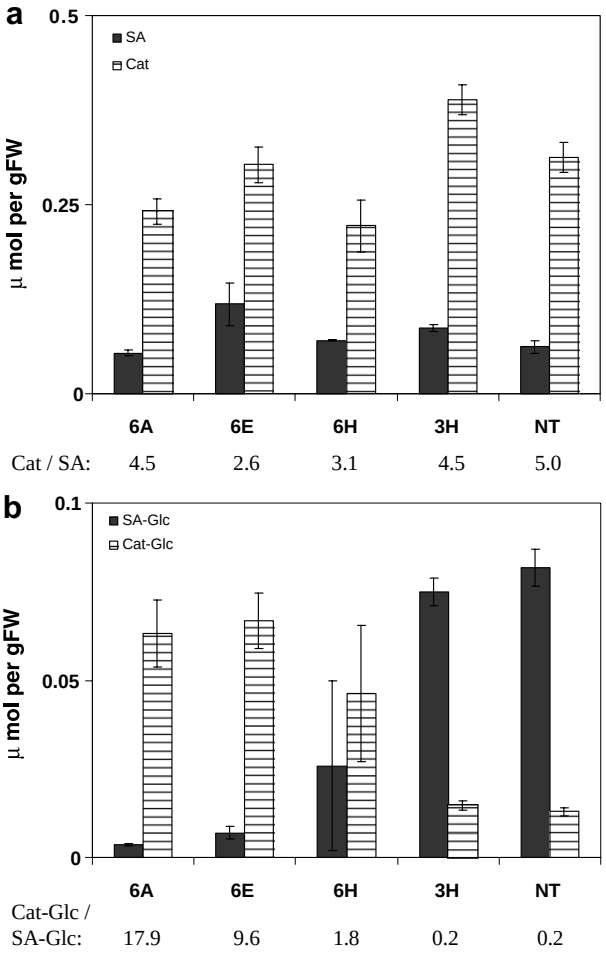

Fig. 2. SA, catechol and glycoside quantitation in *nahG* transgenic lines. (a) Ratios of catechol (Cat) to SA and (b) catechol glucoside (Cat-Glc) to SA glycoside (SA-Glc) given in μmol of glucose equivalents per gram fresh weight ± SE for three biological replicates. Note scale differences.

metabolic pathways that compensate for the removal of SA **1** by *nahG*. In this scenario, converting SA **1** to catechol **2** through the action of the *nahG* transgene would alter the activities of endogenous enzymes, leading to increased SA **1** biosynthesis or release of SA **1** from a storage form, and thus to the maintenance of SA **1** and catechol **2** pools.

2.3. Metabolic profiling reveals alteration in secondary metabolism in nahG transgenics

To test the hypothesis that the stability of SA **1** levels in the transgenic lines is due to shifts in enzyme activities that generate altered levels of compounds other than SA **1** and catechol **2**, GC–MS was used to measure additional secondary metabolites in *nahG* and NT lines. Out of a total of approximately 240 compounds that were detected, we focused on 40 compounds, including SA **1** and catechol **2**, that appeared different in abundance between transgenic and non-transgenic lines (Table 1). The majority of metabolites (32 out of 40) were identified by comparing their mass spectra and retention indices to those available for reference compounds. The eight compounds for which exact structures could not be determined are referred to by their retention index followed by one or more of their key mass/charge (m/z) ratios. Because measurements were made on leaf samples that were pooled from LPI 0 to LPI 8, these single time point data reflect average values during leaf development. Analysis of variance and Dunnett's two-tailed mean comparison tests to compare each transgenic line to the NT control identified 36 significant metabolites at $P < 0.10$, 31 at $P < 0.05$, and 17 at $P < 0.01$ whose concentrations were significantly altered between a given *nahG* transgenic line and the NT control.

Consistent with the hypothesis that alterations in secondary metabolic pathways that do not directly involve SA **1** are modified, the pool size of glycosyl-conjugated SA **4** in two of the high-expressing *nahG* lines (6A and 6E) was reduced to 4.3% and 8.5% of the control, respectively (Fig. 2b). In contrast, the pool size of glycosyl-conjugated SA **4** in the low-expressing *nahG* line 3H was only slightly less than the control (91.8% of NT; Fig. 2b). The pool sizes of glycosyl-conjugated catechol **3** in lines 6A and 6E increased approximately 5-fold relative to the control and line 3H (Fig. 2b). Thus, the level of glycosyl-

Table 1
Quantitative determination of metabolite concentrations (μmol glucose equivalent/g FW) in transgenic poplar

Metabolite ID[a]	6A		6E		6H		3H		NT	
	Mean	SE[b]	Mean	SE[b]	Mean	SE[b]	Mean	SE[b]	Mean	SE[b]
3-*O*-Caffeoyl-quinic acid	2.026	0.203	2.169	0.137	1.806	0.192	3.105	0.159	3.195	0.052
3-*O*-Coumaroyl-quinic acid	0.449	0.042	0.445	0.022	0.383	0.062	0.678	0.060	0.621	0.028
3-*O*-Feruloyl-quinic acid	0.088	0.002	0.089	0.003	0.069	0.005	0.109	0.006	0.114	0.003
4-*O*-Caffeoyl-quinic acid	0.604	0.030	0.590	0.044	0.519	0.051	0.618	0.002	0.876	0.055
4-*O*-Coumaroyl-quinic acid	0.237	0.029	0.256	0.010	0.211	0.024	0.276	0.010	0.333	0.019
4-*O*-Feruloyl-quinic acid	0.027	0.000	0.034	0.002	0.030	0.003	0.033	0.002	0.046	0.003
5-*O*-Caffeoyl-quinic acid	0.592	0.008	0.566	0.064	0.499	0.041	0.636	0.058	0.981	0.030
5-*O*-Coumaroyl-quinic acid	0.293	0.010	0.284	0.018	0.231	0.027	0.365	0.029	0.463	0.018
5-*O*-Feruloyl-quinic acid	0.153	0.010	0.170	0.013	0.131	0.005	0.143	0.005	0.187	0.013
Arbutin	0.006	0.000	0.005	0.000	0.005	0.001	0.006	0.000	0.008	0.000
Caffeic acid	0.163	0.008	0.229	0.032	0.155	0.003	0.189	0.014	0.186	0.021
(+)-Catechin	0.185	0.027	0.122	0.030	0.180	0.097	0.637	0.085	0.759	0.022
Catechol	0.241	0.017	0.303	0.023	0.222	0.034	0.389	0.019	0.313	0.020
Catechol glucoside	0.063	0.009	0.067	0.008	0.046	0.019	0.015	0.001	0.013	0.001
Coniferin	0.003	0.000	0.001	0.001	0.002	0.001	0.004	0.000	0.005	0.000
p-Coumaric acid	0.076	0.005	0.087	0.005	0.067	0.005	0.094	0.003	0.087	0.005
Coumaric acid glucoside	0.451	0.011	0.581	0.125	0.532	0.039	0.669	0.038	0.465	0.203
Dicoumaric acid glycoside	0.037	0.010	0.055	0.000	0.058	0.016	0.055	0.011	0.073	0.004
Ferulic acid	0.016	0.000	0.018	0.001	0.011	0.002	0.019	0.001	0.021	0.002
Feruloyl-glucoside	0.081	0.003	0.112	0.012	0.080	0.010	0.122	0.005	0.123	0.009
Hydroquinone	0.039	0.002	0.068	0.018	0.059	0.014	0.053	0.013	0.060	0.020
Phytol	1.092	0.044	1.397	0.065	1.001	0.115	1.609	0.080	1.676	0.073
Quinic acid	8.811	0.263	13.210	0.996	9.275	0.348	13.939	0.399	10.644	0.401
Salicin	2.011	0.139	2.758	0.260	2.107	0.376	4.014	0.154	2.883	0.064
Salicortin	8.954	0.381	14.665	0.921	9.566	1.054	13.877	0.153	11.054	0.631
Salicyl alcohol	0.024	0.001	0.035	0.005	0.022	0.005	0.040	0.005	0.040	0.000
Salicylic acid	0.054	0.004	0.118	0.028	0.071	0.001	0.087	0.004	0.062	0.008
Salicylic acid glucoside	0.004	0.000	0.007	0.002	0.026	0.024	0.075	0.004	0.082	0.005
B-sitosterol	0.256	0.003	0.265	0.008	0.258	0.038	0.340	0.023	0.354	0.029
Syringin	0.009	0.001	0.008	0.002	0.009	0.004	0.017	0.002	0.018	0.001
Tremuloidin	0.041	0.004	0.061	0.004	0.050	0.009	0.067	0.002	0.067	0.009
Triandrin	0.041	0.003	0.043	0.002	0.034	0.011	0.068	0.011	0.086	0.007
1351.2_184, 285	1.493	0.159	1.903	0.166	1.386	0.190	2.231	0.240	1.340	0.128
2618.8_285 glucoside	1.031	0.035	1.375	0.063	1.055	0.101	1.411	0.043	1.409	0.100
2833_370, 355 phenolic glucoside	0.133	0.015	0.184	0.031	0.177	0.071	0.352	0.040	0.388	0.017
3063.8_297 phenolic glucoside	0.051	0.002	0.060	0.003	0.057	0.012	0.087	0.005	0.088	0.007
3081.1_324, 297 phenolic glucoside	0.039	0.003	0.046	0.002	0.045	0.011	0.069	0.004	0.071	0.005
3108.7_333 phenolic glycoside	0.161	0.015	0.188	0.002	0.177	0.023	0.226	0.020	0.268	0.016
3129.8_354, 297 phenolic glucoside	0.009	0.001	0.010	0.001	0.010	0.003	0.015	0.001	0.016	0.001
3208.3_330, 315 phenolic glucoside	0.100	0.009	0.153	0.007	0.143	0.026	0.163	0.005	0.196	0.022

[a] Metabolite IDs for unknowns are denoted by retention index_key *m/z* fragment(s) and compound class.
[b] SE, standard error.

conjugated SA **4** was negatively correlated to transgene expression while the level of glycosyl-conjugated catechol **3** was positively correlated. The additional catechol glycoside **3** levels associated with the *nahG* transgene may reflect a glycosyltransferase mediated detoxification response to catechol **2** synthesized from SA **1** in an inappropriate cellular location (reviewed in Bowles et al., 2006). However, we note that the level of catechol in its conjugated form is low in proportion to the free catechol **2** (Fig. 2b). These results suggest that poplar cells sustain SA **1** and catechol **2** at consistent levels such that the *nahG* phenotype is characterized by changes in the levels of metabolites outside of the specific enzymatic step it regulates (Fig. 2a and b), with glycoside conjugates acting as potential pools for the product and substrate of the nahG enzyme, respectively. Since consistent SA **1** and catechol **2** concentrations are maintained, we conclude that there may be a biological function that relies on consistent levels of SA **1**, catechol **2**, or both in poplar trees.

A clustergram was constructed by clustering the least square means for the 31 metabolites identified as significantly different between the indicated transgenic line and the control at $P < 0.05$ (vertical dimension, Fig. 3) for each given contrast or comparison (horizontal dimension, Fig. 3). The metabolic response of 3H, the lowest *nahG*-expressing line, was predominantly a subset of the responses seen in the higher-expressing lines while the higher *nahG*-expressing lines had higher numbers of significantly regulated metabolites (Fig. 3). This indicates that increased *nahG* expression leads to increased changes in

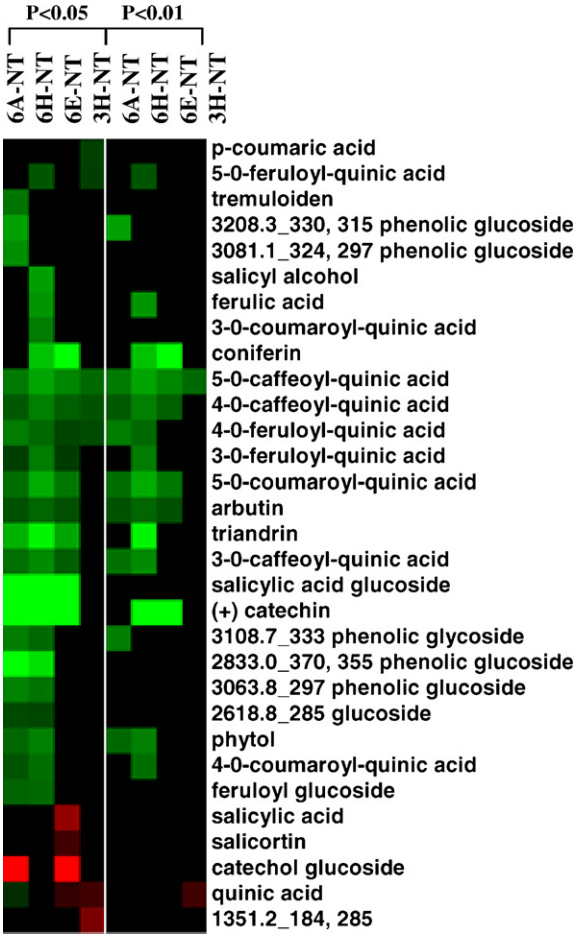

Fig. 3. Clustergram of metabolites significantly regulated in *nahG* transgenic lines contrasted to the non-transgenic control (NT). Contrasts in which metabolites are elevated (red) or repressed (green) are shown at $P < 0.05$ and $P < 0.01$ significance levels. Color intensities correspond to relative least square means values obtained by Dunnett's adjustment test from $\log_2$-converted data with higher color intensities indicating higher deviations from the NT. Non-significant contrasts are in black.

metabolites. Interestingly, the phenolic compounds reduced in *nahG*-3H did not include salicylate derivatives but were comprised mainly of quinic acid conjugated to lignin precursors, compounds also significantly reduced in the other three lines.

Since a positive relationship is visible between increased *nahG* expression and increased metabolite changes (Figs. 2b and 3) and we observe consistent metabolic shifts in multiple independent *nahG* transgenic lines, we conclude that *nahG* transgene expression is driving the alterations in metabolite pools in the transgenic lines. This relationship suggests that the significantly regulated metabolites are co-regulated and therefore connected by underlying biochemical pathways. To explore the relationships among altered metabolites, we calculated Pearson product moment correlations (r) between all pairs of significant metabolites (Steuer et al., 2003). As expected, metabolite-metabolite scatter-plots with strong observable linear relationships had r values closer to 1.0 than did scatter-plots with weaker relationships (Fig. 4a and b). For example, a strong linear relationship was observed between two unknown phenolic glucosides (with retention index_m/z ratio of 3063.8_297 and 3081.1_324, 297) (Fig. 4a) while a weaker relationship was seen between SA **1** and quinic acid **5** (Fig. 4b). An r value of −0.9436 for glycosyl-conjugated catechol and glycosyl-conjugated SA confirmed the positive relationship visible in Fig. 2b. In contrast, the r value between SA and catechol was 0.5032; if the transgene exerted its predicted effect, we would expect a high negative correlation (i.e. depletion of SA coupled with enrichment of catechol).

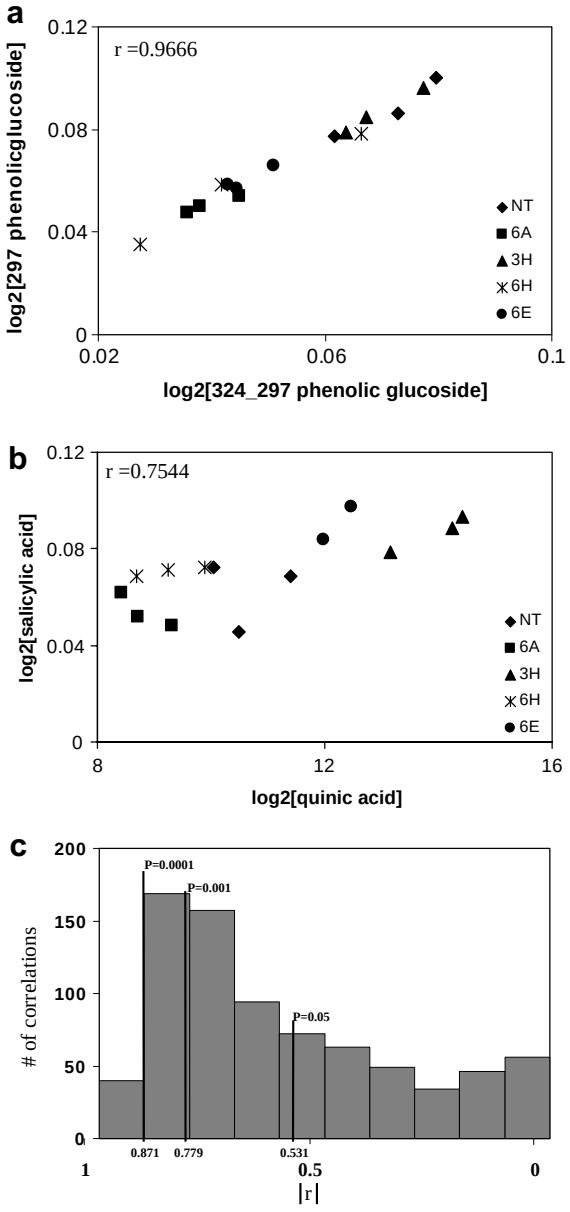

Fig. 4. Scatterplots and Pearson correlations between significant metabolites. Scatter plots of the associations for (a) 3081.1_324, 297 phenolic glucoside by 3063.8_297 phenolic glucoside and (b) salicylic acid by quinic acid, were plotted using the $\log_2$ concentrations (μmol glucose equivalents/gFW) for each plant (three biological replicates/transgenic line). Pearson correlation coefficients are indicated (r). (c) Histogram showing the distribution of the absolute value of the Pearson correlation coefficient (r) among metabolites. P values are indicated.

Shifts in the levels of significantly altered metabolites were non-random, as indicted by the distribution of the absolute values for *r*. Non-coordinately regulated metabolites would show a correlation centered on a zero mean. In contrast, the skewed distribution of the correlations among metabolites (Fig. 4c) reveals that, of the 780 pairwise correlations calculated, 47% (366) are greater than 0.7. In fact, 9 of the 17 metabolites significant at $P < 0.01$ include quinic acid or quinate conjugates (8) and therefore are presumed to be located in the same or in highly related metabolic pathways. Additionally, three compounds are glycosylated phenolic compounds (arbutin **6**, coniferin **7** and triandrin **8**), one is an acyclic terpenoid (phytol **9**), two are unknowns (3108.7_333 phenolic glycoside and 3208.3_330, 315 phenolic glucoside) and the final two are ferulic acid **10** (a lignin precursor), and a flavanol ((+) catechin **11**). The finding that approximately one-half of the highly significant metabolites are quinic acid conjugates, while the other half consists of various phenolic compounds suggests tuning of the shikimate (the source of quinic acid and aromatic amino acids) and phenylpropanoid (the source of lignin precursors) pathways in the *nahG*-expressing lines.

2.4. Whole-plant phenotypes are not apparent

We performed a variety of experiments in which *nahG* and NT plants were propagated and then phenotyped in order to identify whole-plant, organ-level or molecular-level differences between them. We detected no whole-plant differences in propagation efficiency, growth rate, plant architecture or plant size under normal greenhouse or growth chamber conditions (Fig. 1b and data not shown). Alterations in phenolic compounds can affect responses to abiotic stresses; plants grown in a growth chamber (low light) and moved outdoors (high light) showed no differential response to the elevated light and UV levels as measured by chlorophyll fluorescence (F_v/F_m) or degree of visible leaf damage (data not shown). Similarly, we found no differences between *nahG* and NT lines in their photosynthetic efficiency as measured by chlorophyll fluorescence after leaf discs were incubated in solutions of paraquat – a strong oxidant – followed by exposure to high light (data not shown). No morphological differences in tissue type distribution were observed in stem sections stained with phloroglucinol (data not shown). Because there is evidence for cross-talk between inducible SA and wound responsive signaling pathways (Kunkel and Brooks, 2002), we tested the effects of *nahG* expression on wound-responsive gene expression using arrays (Lawrence et al., 2006). No significant differences were detected in the number of genes that were induced by wounding, nor in the magnitude of induction of any wound-inducible transcript (data not shown). The lack of a whole-plant phenotype in *nahG* transgenics supports the conclusion that pleiotropic effects of the transgene are unlikely to be responsible for the metabolic phenotypes we observed.

2.5. Concluding remarks

Our results indicate that *Populus* has a high basal level of SA **1** that is unaffected by expression of the *nahG* transgene. This is in contrast to other plant species, such as potato, in which *nahG* transgene expression can reduce high basal levels of total SA **1**, from 5.2 to less than 0.15 μg/g FW (Yu et al., 1997). The data suggest poplars have a mechanism for the maintenance of high constitutive SA **1** levels at the expense of shikimate and phenylpropanoid metabolites. We hypothesize that the shifts in metabolites noted in the transgenic lines may be a consequence of metabolic channeling. Data on phenylpropanoid biosynthesis suggests that the wide range of compounds produced by this pathway and its different branches are regulated by the formation of complexes of enzymes near cellular membranes (reviewed in Winkel-Shirley, 1999; Jorgensen et al., 2005). The physical association of the enzymes in these complexes can thus regulate metabolic flux, direct intermediates to specific metabolic branches, protect the cell from toxic intermediates, and target products to specific subcellular locations. Since the biological activity of a compound is determined, in part, by its distribution within the cell as well as its modification state, knowledge of the cellular and subcellular compartmentation of SA **1**, catechol **2** and their respective glycosides in *Populus* will lead to insights into the mechanisms of how such high levels of potentially autotoxic phenolic compounds are maintained.

Elevated levels of SA **1** may be biologically significant, perhaps in conditioning interactions with other organisms, similar to the role for SA **1** in host-pathogen signaling. The performance of gypsy moths and forest tent caterpillars on *Populus* is strongly influenced by variation in phenolic glycoside levels (Lindroth and Hemming, 1990; Lindroth and Bloomer, 1991; Lindroth and Weisbrod, 1991; Hemming and Lindroth, 1995; Hwang and Lindroth, 1997). Relationships between SA and heavy metal accumulation have been established for *Thlaspi* sp. (Freeman et al., 2005), as well as for monocots (Metwally et al., 2003; Mishra and Choudhuri, 1999; Pal et al., 2005) and both poplars and related willows can accumulate significant amounts of various heavy metals (Robinson et al., 2000, 2005). Although our studies do not illuminate a specific role for elevated SA **1** in poplar, it would appear that high levels may be adaptive.

3. Experimental

3.1. Plant material, transgenesis, and growth conditions

The *nahG* construct was obtained from Leslie Friedrich (Syngenta Biotechnology, Research Triangle Park, NC). Hybrid poplar clone, INRA 717 1-B4 (*P. tremula* × *P. alba*) was placed into sterile culture prior to *Agrobacterium*-mediated transformation of 100 leaf discs (Leple et al., 1992). Individual clones from independent lines were clonally propagated as softwood cuttings under mist, transferred

to 3.8 L pots and grown to a height of 60–100 cm prior to experimentation (Lawrence et al., 1997). Greenhouse conditions ranged from 20 to 35 °C under natural lighting (from May 1 to September 1) or under extended photoperiod using florescent lights (from September 2 to April 31) for day lengths of 12–14 h. At mid-day the light intensity in the greenhouse averaged 500–700 μE/m^2/min PAR, which was one-half the light intensity outside the greenhouse. Plants were fertilized regularly with Peters Professional 20–10–20 adjusted to 4 mM nitrogen.

3.2. RNA gel blot analysis and phenotyping assays

Total RNA was prepared using a CTAB method (Chang et al., 1993). Ten micrograms of total RNA per sample was separated by formaldehyde-agarose gel electrophoresis and RNA blot analyses were performed as described (Cooke et al., 2003).

Phloroglucinol staining: Stems were hand-sectioned just above LPI 3 and LPI 9 for three biological replicates per line (6A, 6E, 3H, 6H and NT control line). Tissue sections were stained for lignin using phloroglucinol/HCl (5% in an ethanol/HCl mix 9:1) and immediately placed under a dissecting microscope for observations of gross morphological features including patterns of lignin deposition and anatomy.

Paraquat treatments: For each line (6A, 6E, 3H and NT), five biological replicates were grown to an average height of 80 cm and randomly assigned to one of five blocks. Fifteen leaf discs (3 cm each) were collected from each LPI 8 leaf and randomly placed in one of five treatments (0, 1, 10, 100, and 1000 μM paraquat; chemical purchased from Sigma Chemical Co., St. Louis, MO, USA). Leaf discs were incubated for 2 h in the dark to allow paraquat uptake followed by transfer to the light. Chlorophyll fluorescence (F_v/F_m) was measured every 2 h over a 6 h time period with a portable photosynthesis system (LI-6400, Li-Cor, Lincoln, NE).

UV treatment: For each line (6A, 6E, 3H, and NT) five biological replicates were propagated and grown to an average height of 75 cm in a growth chamber (12 h photoperiod, full-spectrum fluorescent light, 200–300 μE/m^2/min PAR). Chlorophyll fluorescence (F_v/F_m) was measured on a leaf at LPI 8 using the LI-6400 before transfer to direct sunlight (1400 μE/m^2/min PAR). All LPI 8 leaves were oriented southward after transfer to full sun and measurements taken 2 h and 6 h after transfer. After the second measurement, plants were returned to the growth chamber for 3 h prior to a final measurement to assay photosynthetic recovery.

3.3. Metabolic profiling: extraction, separation and identification

For metabolic profiling by GC–MS, three biological replicates from each of four selected transgenic lines (6A, 6E, 6H, and 3H) and a NT control line were randomized in the greenhouse and grown to a final height of 75 cm prior to harvesting and pooling LPI 0 to LPI 8 leaf tissues. Metabolites were analyzed in pooled leaf tissues using

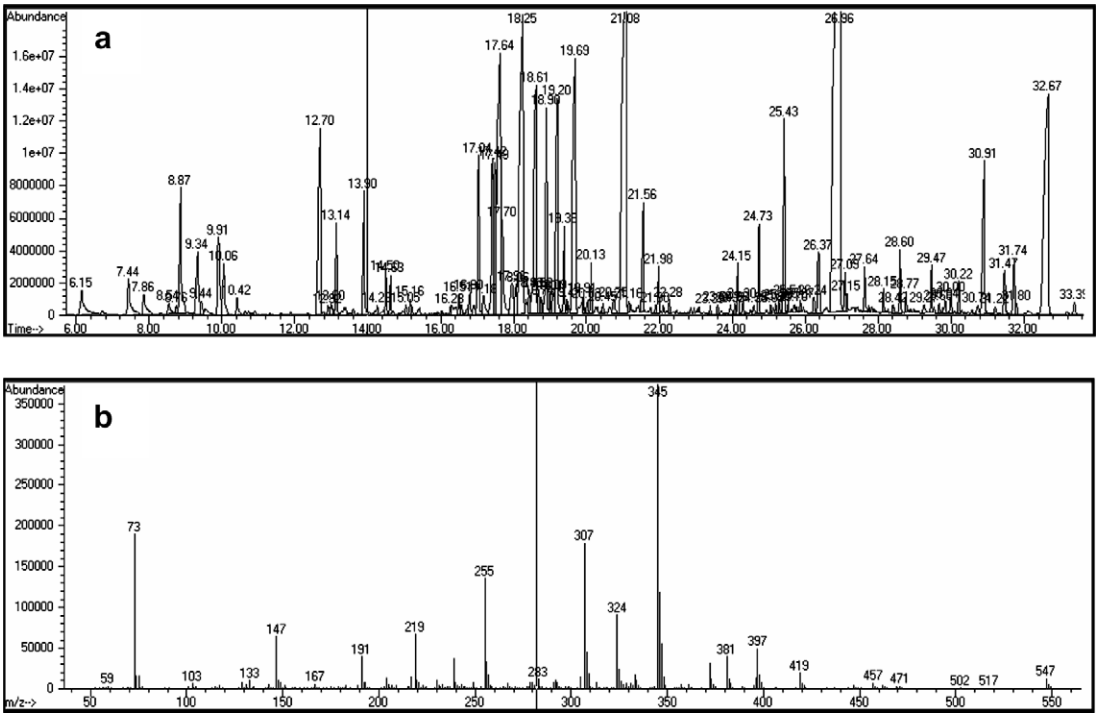

Fig. 5. An example of the GC–MS results. (a) TIC (total ion current) chromatogram produced by MS positive ion detector and the (b) fragmentation pattern for 3-*O*-caffeoyl-quinic acid.

GC–MS where chromatogram peaks were evaluated via their retention times and mass spectra. Leaf samples were flash-frozen in liquid nitrogen and stored at −80 °C until analyzed. After grinding to a fine powder in the presence of dry ice, approximately 300 mg of leaf tissue (fresh weight) were twice extracted with 5 mL of 80% ethanol overnight and then combined prior to drying a 3-mL aliquot in a nitrogen stream. Sorbitol (200 μL of a 1 mg/mL aqueous solution) was added before extraction as an internal standard to correct for differences in extraction efficiency, subsequent differences in derivatization efficiency and changes in sample volume during heating. For generation of trimethylsilyl (TMS) derivatives (Gebre and Tschaplinski, 2002), dried extracts were dissolved in 500 μL silylation-grade acetonitrile followed by 500 μL *N*-methyl-*N*-trimethylsilyltrifluoroacetamide (MSTFA) with 1% trimethylchlorosilane (TMCS) (Pierce Chemical Co., Rockford, IL), and heated for 1 h at 70 °C, with samples injected after 48 h into an HP 5890 Series II gas chromatograph (GC) coupled to an HP 5972 mass spectrometer (MS) (Hewlett–Packard), fitted with an Rtx-5MS (crosslinked 5% PH ME Siloxane) 30 m × 0.25 mm × 0.25 μm film thickness capillary column (Restek). The standard quadrupole GC–MS was operated in electron impact (70 eV) mode, with 1.5 full spectra (50–550 Da) scans per second. Gas (helium) flow was set at 0.6 mL/min with the injection port configured in the splitless mode. The injection port and detector temperatures were set to 250 °C and 300°C, respectively. The initial oven temperature was held at 100 °C for 4 min and was programmed to increase at 8 °C per min to 300 °C where it was held for another 21 min, before cycling to the initial conditions.

All peaks above a set minimum threshold were integrated, whether or not their identity was known. The low abundance peaks that approached statistically significant thresholds (relative to the control plants) were reintegrated and reanalyzed using a key selected ion, characteristic *m*/*z* fragment, rather than the total ion chromatogram, to minimize integrating co-eluting metabolites. Overlapping peaks were manually deconvoluted using relatively unique fragments for each metabolite. A large user-created mass spectral database (>700 metabolites) was used to identify peaks and identify unique fragments for data extraction. Peaks were quantified by area integration and relative concentrations determined based on the quantity of the internal standard (sorbitol) with data then expressed in μmol of glucose equivalents per gram fresh weight. For approximately one third of the metabolites, quantification used the total ion chromatogram (TIC). The remaining two thirds were quantified from an extracted key fragment and concentrations estimated using a correction factor to scale from the extracted ion to the total ion because of skewed peak shapes or additional *m*/*z* fragments indicative of peak overlap. The correction factor was determined from either a standard or from the peak obtained in the first plant sample run in a given sample set that did not indicate the presence of co-eluting interference. Unidentified metabolites are denoted by their key *m*/*z* fragment,

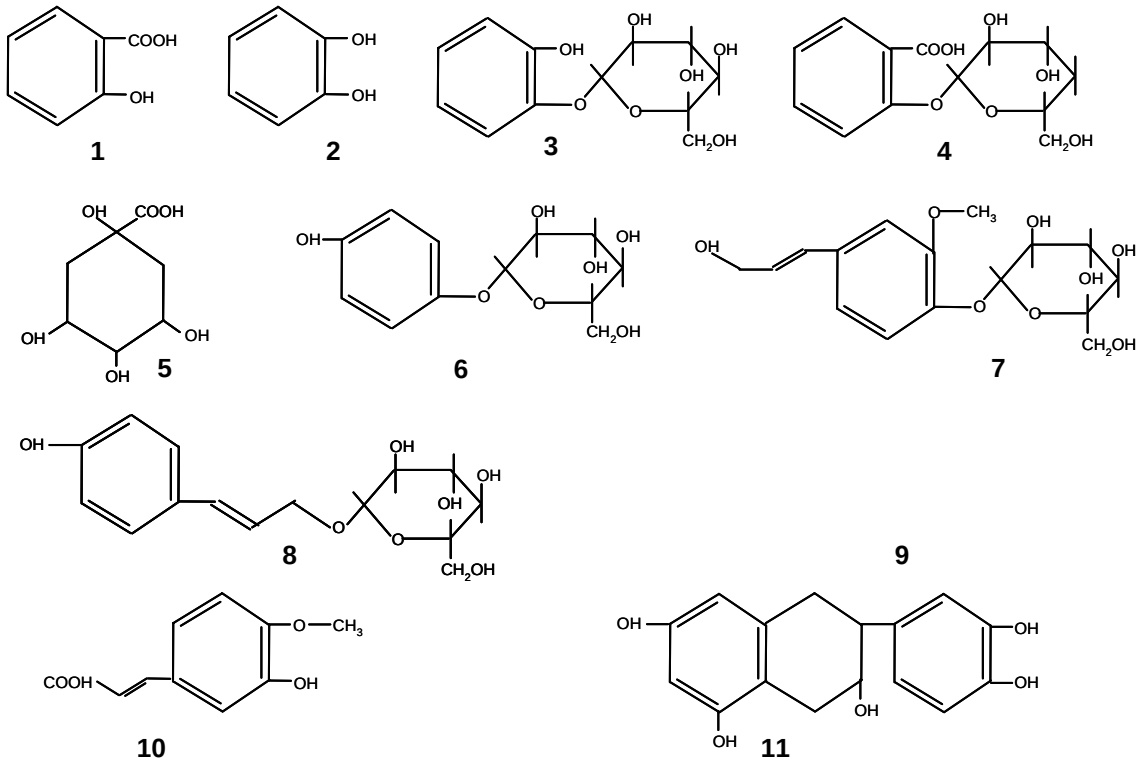

Fig. 6. Structures of selected compounds: salicylic acid **1**, catechol **2**, catechol glucoside **3**, salicylic acid glucoside **4**, quinic acid **5**, arbutin **6**, coniferin **7**, triandrin **8**, phytol **9**, ferulic acid **10**, and (+) catechin **11**.

class of compound and retention index (Schauer et al., 2005; Wagner et al., 2003). Retention indices of unidentified metabolites were determined by interpolation of the retention indices of known metabolites bracketing the unknown, using the average values reported at the Golm Metabolome Database website (http://csbdb.mpimp-golm.mpg.de/csbdb/gmd/profile/gmd_smpq.html). An example of the GC–MS results is shown in Fig. 5 and structures for called out compounds are given in Fig. 6.

3.4. Statistical analysis and clustering

ANOVA, Dunnett's two-tailed tests and correlation analyses were performed in SAS (version 9.1; SAS Institute Cary, NC) to obtain relative least square means values from $\log_2$-converted data and identify statistically significant metabolites. Hierarchical clustering was performed using the Cluster program (Eisen et al., 1998) with the following settings; gene and array cutoff of 0.8, gene and array exponent of 2, uncentered correlation and average linkage clustering. Tree View (Eisen et al., 1998) was used for visualization.

Acknowledgments

The work was supported by Department of Energy award DE-FG-02-04ER63845 and Consortium for Plant Biotechnology Award EPA82947901-128 (to J.D.) and, in part, by the Office of Science, Biological, and Environmental Research, US Department of Energy (to T.J.T.). Oak Ridge National Laboratory is managed by UT-Battelle, LLC, for the US Department of Energy under contract DE-AC05-00OR22725. We sincerely thank Katherine Smith for help with plant maintenance and harvesting; Dudley Huber and Tania Quesada for assistance with statistical analyses; and Timothy Martin for light measurements, chlorophyll fluorescence measurements, and helpful discussions. We gratefully acknowledge Syngenta Biotechnology Inc. for their gift of the *nahG* construct.

References

Allen, J., Davey, H.M., Broadhurst, D., Heald, J.K., Rowland, J.J., Oliver, S.G., Kell, D.B., 2003. High-throughput classification of yeast mutants for functional genomics using metabolic footprinting. Nature Biotechnology 21 (6), 692–696.

Bowles, D., Lim, E.K., Poppenberger, B., Vaistij, F.E., 2006. Glycosyltransferases of lipophilic small molecules. Annual Review of Plant Biology 57, 567–597.

Busov, V., Meilan, R., Pearce, D.W., Rood, S.B., Ma, C.P., Tschaplinski, T.J., Strauss, S.H., 2006. Transgenic modification of *gai* or *rgl1* causes dwarfing and alters gibberellins, root growth, and metabolite profiles in *Populus*. Planta 224 (2), 288–299.

Chang, S., Puryear, J., Cairney, J., 1993. A simple and efficient method of isolating RNA from pine trees. Plant Molecular Biology Reporter 11, 113–116.

Chini, A., Grant, J.J., Seki, M., Shinozaki, K., Loake, G.J., 2004. Drought tolerance established by enhanced expression of the CC-NBS-LRR gene, *ADR1*, requires salicylic acid, EDS1 and ABI1. Plant Journal 38 (5), 810–822.

Cooke, J.E.K., Brown, K.A., Wu, R., Davis, J.M., 2003. Gene expression associated with N-induced shifts in resource allocation in poplar. Plant Cell and Environment 26 (5), 757–770.

Cutler, S., McCourt, P., 2005. Dude, where's my phenotype? Dealing with redundancy in signaling networks. Plant Physiology 138 (2), 558–559.

Delaney, T.P., Uknes, S., Vernooij, B., Friedrich, L., Weymann, K., Negrotto, D., Gaffney, T., Gutrella, M., Kessmann, H., Ward, E., Ryals, J., 1994. A central role of salicylic-acid in plant-disease resistance. Science 266 (5188), 1247–1250.

Eisen, M.B., Spellman, P.T., Brown, P.O., Botstein, D., 1998. Cluster analysis and display of genome-wide expression patterns. Proceedings of the National Academy of Sciences of the United States of America 95 (25), 14863–14868.

Freeman, J.L., Garcia, D., Kim, D., Hopf, A., Salt, D.E., 2005. Constitutively elevated salicylic acid signals glutathione-mediated nickel tolerance in *Thlaspi* nickel hyperaccumulators. Plant Physiology 137 (3), 1082–1091.

Friedrich, L., Vernooij, B., Gaffney, T., Morse, A., Ryals, J., 1995. Characterization of tobacco plants expressing a bacterial salicylate hydroxylase gene. Plant Molecular Biology 29 (5), 959–968.

Gaffney, T., Friedrich, L., Vernooij, B., Negrotto, D., Nye, G., Uknes, S., Ward, E., Kessmann, H., Ryals, J., 1993. Requirement of salicylic-acid for the induction of systemic acquired-resistance. Science 261 (5122), 754–756.

Gebre, G.M., Tschaplinski, T.J., 2002. Solute accumulation of chestnut oak and dogwood leaves in response to through fall manipulation of an upland oak forest. Tree Physiology 22 (4), 251–260.

Heck, S., Grau, T., Buchala, A., Metraux, J.P., Nawrath, C., 2003. Genetic evidence that expression of NahG modifies defence pathways independent of salicylic acid biosynthesis in the Arabidopsis-*Pseudomonas syringae* pv. *tomato* interaction. Plant Journal 36 (3), 342–352.

Hemming, J.D.C., Lindroth, R.L., 1995. Intraspecific variation in aspen phytochemistry: effects on performance of gypsy moths and forest tent caterpillars. Oecologia 103, 79–88.

Hwang, S.Y., Lindroth, R.L., 1997. Clonal variation in foliar chemistry of aspen: effects on gypsy moths and forest tent caterpillars. Oecologia 111, 99–108.

Jorgensen, K., Rasumssen, A.V., Morant, M., Nielsen, A.H., Bjarnholt, N., Zagrobelny, M., Bak, S., Lindberg, B., 2005. Metabolon formation and metabolic channeling in the biosynthesis of plant natural products. Current Opinions in Plant Biology 8 (3), 280–281.

Julkunen-Tiitto, M.R.K., 1989. Phenolic constituents of *Salix*: a chemotaxic survey of further Finnish species. Phytochemistry 28 (8), 2115–2125.

Kunkel, B.N., Brooks, D.M., 2002. Cross talk between signaling pathways in pathogen defense. Current Opinion in Plant Biology 5 (4), 325–331.

Lawrence, S.D., Greenwood, J.S., Korhnak, T.E., Davis, J.M., 1997. A vegetative storage protein homolog is expressed in the growing shoot apex of hybrid poplar. Planta 203 (2), 237–244.

Lawrence, S.D., Dervinis, C., Novak, N., Davis, J.M., 2006. Wound and insect herbivory responsive genes in poplar. Biotechnology Letters 28 (18), 1493–1501.

Lindroth, R.L., Hemming, J.D.C., 1990. Responses of the gypsy moth (Lepidoptera: Lymantriidae) to tremulacin, an aspen phenolic glycoside. Environmental Entomology 19, 842–847.

Lindroth, R.L., Bloomer, M.S., 1991. Biochemical ecology of the forest tent caterpillar: responses to dietary protein and phenolic glycosides. Oecologia 86, 408–413.

Lindroth, R.L., Weisbrod, A.V., 1991. Genetic variation in response of the gypsy moth to aspen phenolic glycosides. Biochemical Systematics and Ecology 19, 97–103.

Leple, J.C., Brasileiro, A.C.M., Michel, M.F., Delmotte, F., Jouanin, L., 1992. Transgenic poplars – expression of chimeric genes using 4 different constructs. Plant Cell Reports 11 (3), 137–141.

Metraux, J.P., 2002. Recent breakthroughs in the study of salicylic acid biosynthesis. Trends in Plant Science 7 (8), 332–334.

Metwally, A., Finkerneier, I., Georgi, M., Dietz, K.J., 2003. Salicylic acid alleviates the cadmium toxicity in barley seedlings. Plant Physiology 132 (1), 272–281.

Mishra, A., Choudhuri, M.A., 1999. Effects of salicylic acid on heavy metal-induced membrane deterioration mediated by lipoxygenase in rice. Biologia Plantarum 42 (3), 409–415.

Morris, K., Mackerness, S.A.H., Page, T., John, C.F., Murphy, A.M., Carr, J.P., Buchanan-Wollaston, V., 2000. Salicylic acid has a role in regulating gene expression during leaf senescence. Plant Journal 23 (5), 677–685.

Orvar, B.L., McPherson, J., Ellis, B.E., 1997. Pre-activating wounding response in tobacco prior to high-level ozone exposure prevents necrotic injury. Plant Journal 11 (2), 203–212.

Pal, M., Horvath, E., Janda, T., Paldi, E., Szalai, G., 2005. Cadmium stimulates the accumulation of salicylic acid and its putative precursors in maize (*Zea mays*) plants. Physiologia Plantarum 125 (3), 356–364.

Pearl, I.A., Darling, S.F., 1971. Phenolic extractives of leaves of *Populus balsamifera* and of *P. trichocarpa*. Phytochemistry 10 (11), 2844.

Raamsdonk, L.M., Teusink, B., Broadhurst, D., Zhang, N., Hayes, A., Walsh, M.C., Berden, J.A., Brindle, K.M., Kell, D.B., Rowland, J.J., Westerhoff, H.V., van Dam, K., Oliver, S.G., 2001. A functional genomics strategy that uses metabolome data to reveal the phenotype of silent mutations. Nature Biotechnology 19 (1), 45–50.

Robinson, B.H., Mills, T.M., Petit, D., Fung, L.E., Green, S.R., Clothier, B.E., 2000. Natural and induced cadmium-accumulation in poplar and willow: implications for phytoremediation. Plant and Soil 227 (1–2), 301–306.

Robinson, B., Mills, T., Green, S., Chancerel, B., Clothier, B., Fung, L., Hurst, S., McIvor, I., 2005. Trace element accumulation by poplars and willows used for stock fodder. New Zealand Journal of Agricultural Research 48 (4), 489–497.

Schauer, N., Steinhauser, D., Strelkov, S., Schomburg, D., Allison, G., Moritz, T., Lundgren, K., Roessner-Tunali, U., Forbes, M.G., Willmitzer, L., Fernie, A.R., Kopka, J., 2005. GC–MS libraries for the rapid identification of metabolites in complex biological samples. FEBS Letters 579 (6), 1332–1337.

Steuer, R., Kurths, J., Fiehn, O., Weckwerth, W., 2003. Observing and interpreting correlations in metabolomic networks. Bioinformatics 19 (8), 1019–1026.

Thieme, H., Benecke, R., 1971. Studies on glycoside accumulation in some central European *Populus* species. Pharmazie 26 (4), 227.

Uknes, S., Winter, A.M., Delaney, T., Vernooij, B., Morse, A., Friedrich, L., Nye, G., Potter, S., Ward, E., Ryals, J., 1993. Biological induction of systemic acquired-resistance in *Arabidopsis*. Molecular Plant–Microbe Interactions 6 (6), 692–698.

van Wees, S.C.M., Glazebrook, J., 2003. Loss of non-host resistance of Arabidopsis NahG to *Pseudomonas syringae* pv. *phaseolicola* is due to degradation products of salicylic acid. Plant Journal 33 (4), 733–742.

Wagner, C., Sefkow, M., Kopka, J., 2003. Construction and application of a mass spectral and retention time index database generated from plant GC/EI-TOF-MS metabolite profiles. Phytochemistry 62 (6), 887–900.

Winkel-Shirley, B., 1999. Evidence for enzyme complexes in the phenylpropanoid and flavonoid pathways. Physiologia Plantarum 107, 142–149.

Weckwerth, W., Loureiro, M.E., Wenzel, K., Fiehn, O., 2004. Differential metabolic networks unravel the effects of silent plant phenotypes. Proceedings of the National Academy of Sciences of the United States of America 101 (20), 7809–7814.

Yu, D.Q., Liu, Y.D., Fan, B.F., Klessig, D.F., Chen, Z.X., 1997. Is the high basal level of salicylic acid important for disease resistance in potato? Plant Physiology 115 (2), 343–349.